Investigations on Hydrogen Assisted Cracking of Welded High-Strength Pipes in Gaseous Hydrogen

M. Tröger[1], C. Bosch[1], J.-N. Wiart[2], H. Meuser[3], F.M. Knoop[4], H. Brauer[5], J. Schröder[6]

① Salzgitter Mannesmann Forschung, Duisburg, Germany
② Salzgitter Mannesmann Precision, Saint-Florentin, France
③ Salzgitter Mannesmann Grobblech, Mühlheim, Germany
④ Salzgitter Mannesmann Großrohr, Salzgitter, Germany
⑤ Salzgitter Mannesmann Line Pipe, Hamm, Germany
⑥ Europipe GmbH, Mühlheim, Germany

ABSTRACT

Four different actual linepipe steels of grade X70 and X80 have been investigated to evaluate the suitability of welded high-strength pipes for hydrogen transport with respect to their resistance to hydrogen embrittlement and hydrogen assisted cracking. The experimental approach includes the analysis of hydrogen uptake using carrier gas hot extraction and slow strain rate tests (SSRT) to investigate the behavior of the materials under expected service conditions.

SSRT results have been evaluated with regard to the maximum stress and ductility parameters such as plastic elongation ratio and reduction in area ratio which were calculated from tests performed under 80 bar gaseous hydrogen and nitrogen as reference. Besides base material, submerged arc welds and high frequency induction welds have been tested. No significant impact of hydrogen on the maximum stress measured for both base material and welds was observed. With values above 80 % the ductility ratios reveal good resistance of the materials to hydrogen assisted cracking. Fractographic analysis of the specimens tested in hydrogen atmosphere presented ductile failure modes for all specimens. Small secondary cracks were detected on specimens of the base material. However, no significant impact of hydrogen on the performance of the material in hydrogen atmosphere was observed under the tested environmental conditions.

KEY WORDS

Slow Strain Rate Tests
Hydrogen transport
Linepipe
HSLA Steels

INTRODUCTION

The growing demand for energy and the need to reduce greenhouse gas emissions motivate the development of alternative energy sources and fuels, especially hydrogen, with transmission and distribution infrastructures as the key challenge.

As an alternative and challenging energy source of the next decades hydrogen gains more and more importance. There are various applications for hydrogen use which are currently discussed. Hydrogen is used in energy source systems for renewable energy technologies. The electrolytic conversion of electricity in hydrogen provides the possibility to store excess power of renewable energy and thus the adaption to current consumer cycles. Another application is the use of hydrogen as “clean” energy carrier for electric mobility.

New fields of application require an infrastructure for transport and storage of gaseous hydrogen. To connect hydrogen production sites with local users, pipelines are generally the first choice.

Lower strength linepipe grades have been widely studied regarding their applicability for hydrogen transport and experience has been gained with existing hydrogen distribution lines. However, experience is generally limited to lower service pressures and linepipes operating with high safety factors to ensure safe operation of the transmission lines without failure. For an economical transport higher mass throughputs are required which can be realized by the use of higher strength materials. An optimal solution for these applications are low alloyed C-Mn steels which are resistant to hydrogen assisted cracking. To ensure a safe transport of gaseous hydrogen the effect of hydrogen has to be carefully studied for standard and high strength pipeline steels.

In the last few years the number of publications and reports dealing with hydrogen assisted cracking of higher strength materials in gaseous hydrogen has increased.

Under static loading no influence of the hydrogen pressure on strength properties has been observed especially for material grades with lower yield strength. However, the ductility has been found to be influenced negatively by the interaction with hydrogen. It was found that under hydrogen charging the fracture toughness and the reduction in area is decreased and that secondary cracks and the area of brittle fracture is increased.[1-7] Similar results have been reported for higher strength materials such as API X80[8] which presented no impact of hydrogen on the yield strength in tensile tests. In contrast to this a significant decrease of the elongation at fracture with decreasing strain rate was observed in the presence of hydrogen. Investigations on lower strength as well as higher strength materials prove that a maximum exists for hydrogen embrittlement with regard to the ductility properties of the materials at a hydrogen partial pressure of 5 - 7 MPa.

In general, the susceptibility of materials to hydrogen embrittlement increases with increasing strength. This is especially the case for material with tensile strengths above 900 MPa. Dynamic loading tests on tensile specimens have shown an increased susceptibility to Hydrogen at and above a tensile stress of about 900 MPa.

In constant extension rate tests (CERT) on low alloyed carbon steels in hydrogen environment crack growth occurred only under continuous or increasing plastic deformation. No influence of

increased hardness in the weld area was observed. The results indicate that hydrogen cracks are only generated under conditions where the material would also fail due to mechanical loading. The presence of small amounts of O_2 or CO has an inhibiting effect and can compensate the detrimental effect of hydrogen almost completely.
The main objective of this project is to evaluate the suitability of high strength pipes for use in hydrogen transport with respect to their resistance to hydrogen assisted cracking. The experimental approach includes the analysis of hydrogen absorption in welded pipes of actual standard grades using hot extraction. In addition, slow strain rate tests were performed on base and weld material to investigate the behavior of the materials under expected environmental conditions.

EXPERIMENTAL PROCEDURE

MATERIAL

For the investigation three linepipe materials of grade X70 derived from different production routes and one material of grade X80 were used. The chemical composition of the materials is given in Table 1.
The X70 materials contain different kinds of welds; the first pipe contains a high frequency induction (HFI) weld (material A), the second pipe is a spiral welded pipe with a submerged arc weld (material B) and the third pipe has a longitudinal submerged arc weld (material C), just like the X80 pipe (material D).
Material A and B show a ferritic pearlitic microstructure while materials C and D show a predominantly bainitic microstructure.

Table 1 – Chemical analysis of investigated materials (mass%)

Material	Grade	C	Si	Mn	P	S	Cu+Ni+Cr+Mo	Nb+V+Ti
A	X70	0.07	0.31	1.4	<0.015	<0.001	<0.4	<0.15
B	X70	0.09	0.34	1.6	<0.015	<0.003	<0.4	<0.15
C	X70	0.05	0.23	1.7	<0.015	<0.001	<0.4	<0.15
D	X80	0.07	0.26	1.9	<0.015	<0.002	<0.4	<0.15

HYDROGEN UPTAKE

For the analysis of hydrogen uptake flat specimens of the dimension 7 x 15 x 60 mm were used. Samples were taken from the base material as well as from the welds. The surface was mechanically ground up to 1000 grit and then electropolished to assure the same surface condition for each specimen.
The specimens were charged in a sour environment with variations in pH and H_2S content. Two different test solutions were used. First was the NACE test solution A specified in NACE TM0177[10] saturated at 1 bar H_2S at a start pH of 2.7. Second was the EFC 16 acetate buffer

solution utilising a gas mixture consisting of 2% H_2S balanced in CO_2 at atmospheric pressure and with a start pH of 3.5. In addition to charging in H_2S containing solution samples were charged electrochemically. Cathodic charging was performed in 0.1 N H_2SO_4 with addition of 10 mg/l As_2O_3 as Hydrogen promoter at a cathodic potential of -1000 mV (SHE).
Hydrogen charging was performed at room temperature for all conditions with charging times of 4 h for the cathodic charging and between 24 and 144 h in case of charging in H_2S solution. After charging the samples were rinsed with ethanol and submerged in liquid nitrogen to avoid desorption of hydrogen prior to the measurement.
The total hydrogen concentration in the materials was determined by effusion using the carrier gas hot extractor H-mat 221 of Juwe Laborgeräte GmbH, Germany. Nitrogen was used as carrier gas. Hydrogen effusion was measured at a constant temperature of 800°C and a measurement time of 20 min.

SLOW STRAIN RATE TESTS (SSRT)

SSRT tests were carried out in hydrogen or nitrogen gas using a dynamic load testing machine Z050 of Zwick Roell, Germany with a test range of 0 - 50 kN. Experiments were performed in a 200 ml autoclave as test vessel. For each material and test condition, 2 specimens were taken longitudinally from the base material and 2 specimens transversely to the weld containing the weld at mid-length. Smooth round bar specimens with a diameter of the gauge section of 6.35 mm and a length of 25.5 mm were tested (Figure 1).

Figure 1 – Test specimen for slow strain rate tests

All specimens were degreased and electropolished before the test start. Prior to testing the test vessel was purged with the test gas to exclude ambient air and humidity.
Slow strain rate tests were performed using two different crosshead speeds corresponding to strain rates of $2.0 \cdot 10^{-6}$ s^{-1} and $2.0 \cdot 10^{-5}$ s^{-1}. Straining was started after pressurizing with 80 bar nitrogen for inert test conditions or with 80 bar hydrogen for the test environment. The purity of the hydrogen gas was ≥ 99,999 Vol.%.
Load vs. strain curves were recorded by load cells connected to the pull rod outside of the autoclave and the signal was processed through an operational amplifier.

The SSRT tests were evaluated by means of the maximum load at failure, reduction in area ratio RAR and plastic elongation ratio EPR defined in NACE TM0198-2004.[10] In order to calculate the reduction in area, the dimensions of the specimens were determined in accordance with NACE TM0198 requirements.
The reduction in area ratio was obtained from the comparison of the reduction in area determined in the test environment with those determined in air by using mean values calculated for each specimen:

$$RAR = \frac{RA_E}{RA_A} \cdot 100\% \quad (1)$$

Where:
RAR = Reduction in area ratio
RA_A = Reduction in area in nitrogen
RA_E = Reduction in area in test environment
As the ductility parameters are calculated from changes in the gauge lengths and diameters during the test, which are measured on the specimens, these parameters are expected to have a certain scatter. This scatter could obscure expected dependencies of these parameters on the performance of the steel in different environments. The plastic elongation (E_P) is determined directly from the load vs. strain curve and is preferred for assessment of the test results as it reduces scatter and allows the comparison to data obtained on different test machines or from different laboratories:

$$E_p(\%) = \left(\frac{V_A t_B}{L_0} - \left[\frac{\sigma_F}{\sigma_p} \right] \frac{V_A t_P}{L_B} \right) \cdot 100\% \quad (2)$$

Where:
v_A = Extension rate in mm/s
t_B = Time-to-failure in s
t_P = Time-to-proportional limit in s
L_0 = Initial gauge length in mm
L_B = Final gauge length in mm
σ_F = Stress at failure
σ_P = Stress at proportional limit
The comparison of the E_P values determined in the test environment E_{PH2} with those determined in nitrogen E_{PN2} was conducted using the plastic elongation ratio (E_PR) as follows:

$$E_PR = \frac{E_{PH2}}{E_{PN2}} \cdot 100\% \quad (3)$$

RESULTS AND DISCUSSION

HYDROGEN UPTAKE

The results of the hydrogen uptake measurements are summarized in Figure 2. In case of material A and C comparable results were obtained for the hydrogen uptake in the welds compared to the base metal while the weld of material B revealed a lower hydrogen solubility. Differences were observed for hydrogen contents after charging in H_2S solution compared to cathodic charging with significantly higher concentrations up to 20 ppm after electrochemical charging. The selected conditions appeared too severe to represent hydrogen uptake in gaseous hydrogen, where much lower hydrogen concentrations are expected, but nonetheless useful to highlight potential differences in hydrogen uptake characteristics of the tested materials. All materials show a higher hydrogen content after charging for 48 h in 100% H_2S solution than for 144 h of charging in the same solution which can be explained by the formation of corrosion product layers which limit hydrogen entry in the material.
Comparing the different materials, highest hydrogen uptake was measured for samples of material B with about 16 ppm, followed by material A with 3.8 ppm and material C with 2.3 ppm for charging in saturated H_2S solution for 48 h. The reason for this difference is supposed to be the higher carbon and sulfur content in material B which could cause a higher amount of MnS inclusions and more distinct segregations. Both are known to act as hydrogen trapping sites.

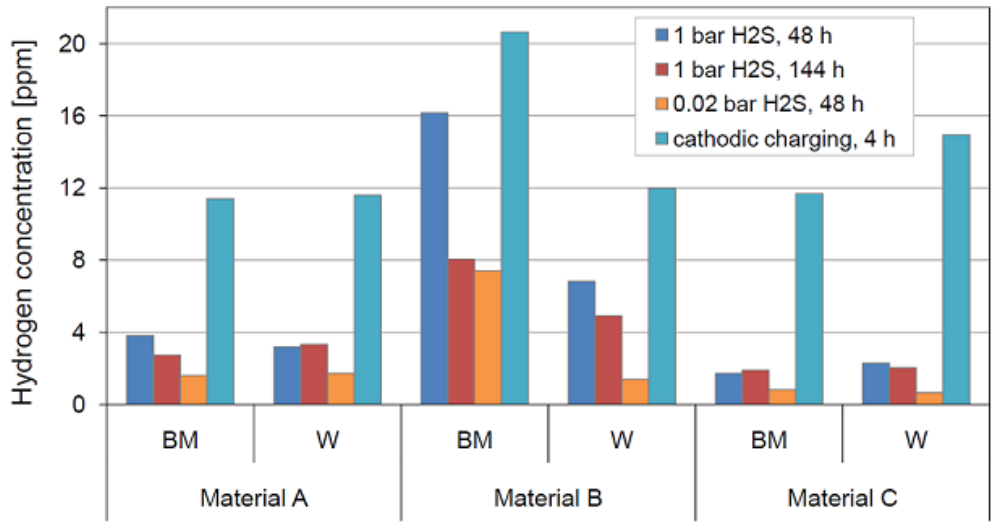

Figure 2 – Comparison of hydrogen content in base material (BM) and weld samples (W)

With regard to the comparability of the tested charging conditions to charging in gaseous hydrogen atmosphere, the 2% H_2S solution seems to be the best solution to approximate the hydrogen uptake behavior of the materials, even though it has to be taken into account that simulating the localized hydrogen uptake and distribution in the steels in gaseous hydrogen atmosphere is not possible by those charging methods.

SLOW STRAIN RATE TESTS (SSRT)

Test results of SSRT tests for all materials are summarized in Table 2 with the calculated ductility parameters RAR and E_PR and the maximum stress load. A comparison of load vs. strain curves of SSRT tests on material C recorded in 80 bar nitrogen or hydrogen are illustrated in Figure 3 for a strain rate of $2.0 \cdot 10^{-5}$ s^{-1}. Results for the higher strength material D are given in Figure 4 recorded at the same strain rate. No clear influence of hydrogen could be observed comparing the tests of material C under inert conditions in nitrogen to the tests in hydrogen atmosphere. The results reveal nearly congruent tensile curves in the two gases for both base material and weld. Small differences for the elongation at failure and the maximum load are independent of the test environment. In case of material D possible small differences for the weld samples could not be confirmed due to some scatter in the test results while the load vs. strain curves of the base material appear to present a slightly different behaviour for tests in nitrogen and hydrogen. Under hydrogen environment the maximum stress load as well as the elongation at failure is lower compared to the results obtained in inert medium.
The calculated ductility ratios RAR and E_PR as well as the maximum load reveal no clear influence of hydrogen for nearly all materials tested (Table 2). The highest deviation was measured for the weld samples of material B with an average reduction of the maximum load of

Table 2 – Results of Slow Strain Rate Tests, BM = base material, W = weld, average values

material	strain rate [s^{-1}]		σ_{max} [N/mm^2]		E_PR [%]	RAR [%]
			N_2	H_2		
A	$2 \cdot 10^{-5}$	BM	607	600	106.1	99.0
		W	588	562		100.5
A	$2 \cdot 10^{-6}$	BM	586	589	103.0	97.1
		W	573	586		96.3
B	$2 \cdot 10^{-5}$	BM	622	618	97.6	98.8
		W	665	536		100.8
C	$2 \cdot 10^{-5}$	BM	545	555	105.3	99.7
		W	554	547		95.5
C	$2 \cdot 10^{-6}$	BM	543	549	97.9	101.3
		W	547	558		102.8
D	$2 \cdot 10^{-5}$	BM	667	626	107.0	99.1
		W	697	669		101.9

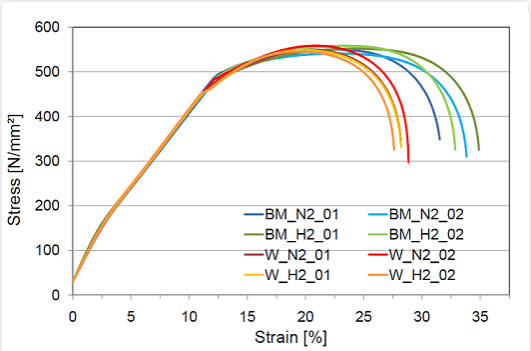

Figure 3 – Load vs. strain curves of material C recorded in 80 bar nitrogen (N_2) and 80 bar hydrogen (H_2), strain rate 2.0 · 10^{-5} s^{-1}, BM = base material, W = weld

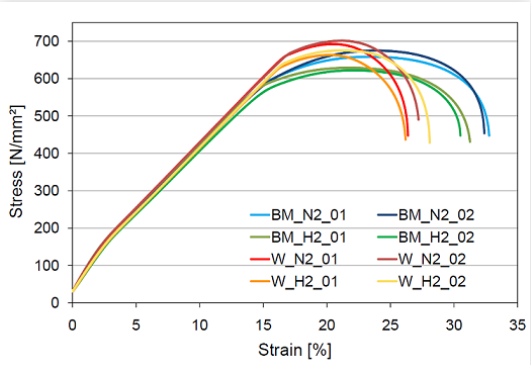

Figure 4 – Load vs. strain curves of material D recorded in 80 bar nitrogen and 80 bar hydrogen, strain rate 2.0 · 10^{-5} s^{-1}, BM = base material, W = weld

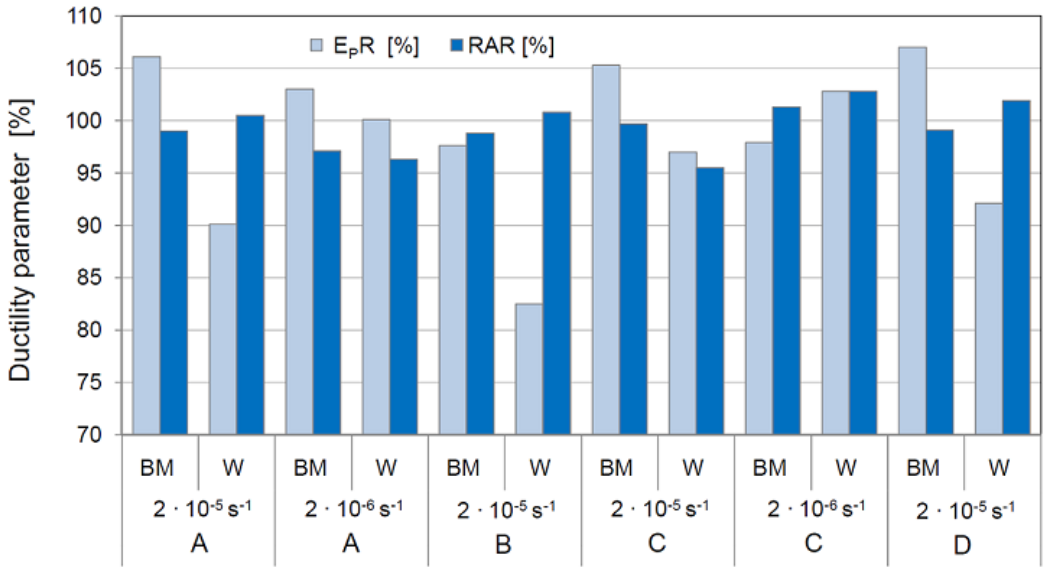

Figure 5 – Plastic elongation ratios E_PR and reduction in area ratios RAR for SSRT tests in 80 bar hydrogen, BM = base material, W = weld

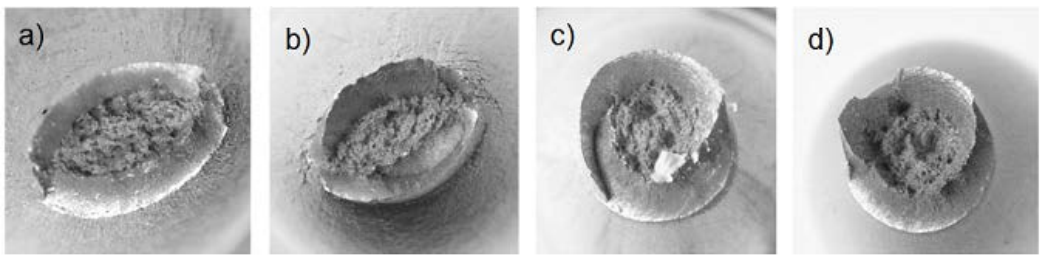

Figure 6 – Fracture surface of tensile specimens after SSRT tests in N_2 or H_2 at a strain rate of 2.0 · 10^{-5} s^{-1}, a) material C - base material in N_2, b) material C - base material in H_2, c) material A - weld in N_2, d) material A - weld in H_2

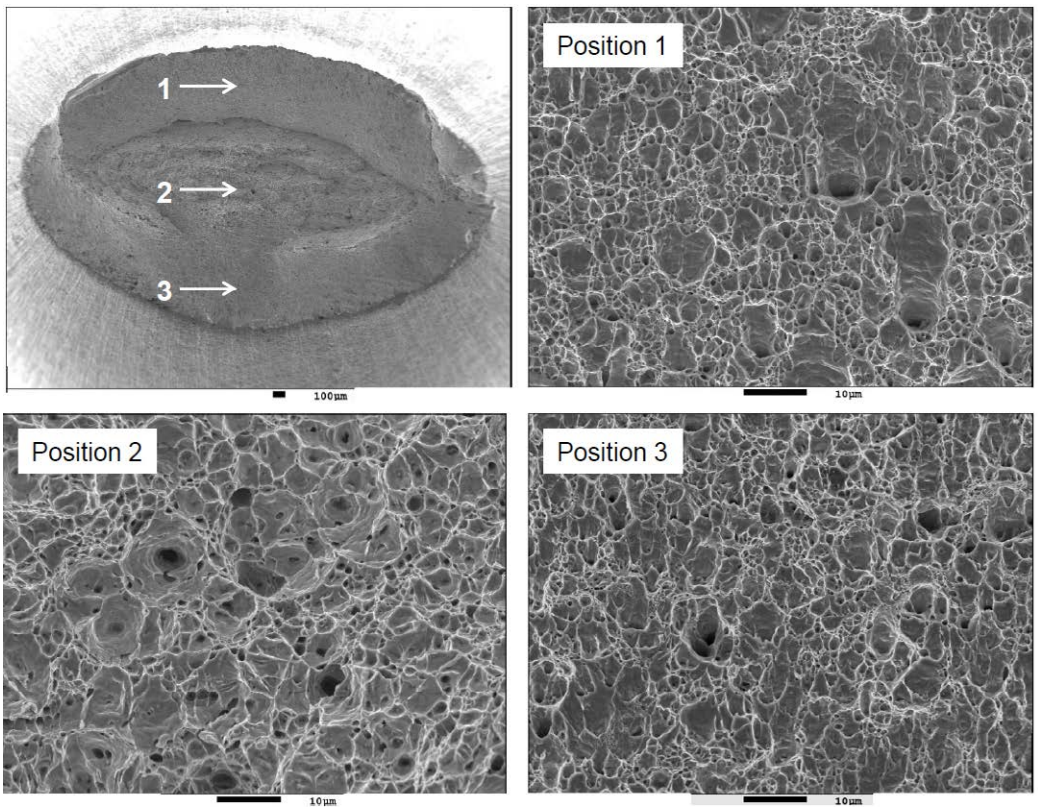

Figure 7 – SEM pictures of the fracture surface of a tensile specimen of material D after SSRT test in H_2 at a strain rate of $2.0 \cdot 10^{-5}$ s^{-1}, base material.

120 N/mm². In case of the higher strength material X80 a reduction of the maximum load of 40 N/mm² was determined for the base material.

For the ductility parameter plastic elongation ratio, values between 90 and 107% were obtained (Figure 5) for nearly all materials indicating a good resistance to hydrogen environmental embrittlement in the tested environment. Comparable values with ratios between 95 and 103% were determined for the reduction in area ratio (Figure 5). Lowest values were obtained for the welds of material B with a ratio of 82.5 % and of material A with a ratio of 90.1%.

In general, values of ductility ratios above 80 % indicate high resistance to environmental cracking.

No influence of the strain rate was observed regarding the materials behaviour in hydrogen atmosphere. In addition, test results for material D indicate a high resistance to hydrogen assisted cracking also for higher strength materials of grade X80.

Fractographic analysis of the SSRT specimens confirms the results obtained for the ductility parameters. All specimens revealed typical ductile failure and no indication of the presence of hydrogen embrittlement at the fracture surface (Figure 6). Some of the specimens show an elliptical fracture as an indication of the texture of the microstructure (Figure 6 a-b). One specimen of material C of the base material show small secondary cracks in the gauge area

in the vicinity of the fracture indicating first signs of embrittlement of the material under plastic strain in pressurized hydrogen (Figure 6 b). Some of the specimens were examined in the SEM confirming the results of the macroscopic examination. Figure 7 shows the fracture surface of a test specimen of material D tested in hydrogen gas. The pictures reveal a ductile failure mode with no evidence of embrittlement.
In order to determine the location of fracture for the weld seam specimens (within the weld metal, heat affect zone or base material), the samples were etched for 30 s in 10% HNO_3.
As expected, the fracture position was located in the heat affected zone (HAZ) which could be explained by the lower hardness in the HAZ compared to weld and base material.

CONCLUSION

Four different linepipe steels of grade X70 and X80 have been investigated to evaluate the suitability of welded high-strength pipes for hydrogen transport with respect to their resistance to hydrogen embrittlement and hydrogen assisted cracking.
The measurements of the hydrogen uptake by hot extraction reveal hydrogen concentrations between 1.7 and 3.8 ppm for materials A and C which are typical values for linepipe materials after exposure in NACE A solution saturated at 1 bar H_2S. Material B presented a significantly higher hydrogen uptake of up to 16 ppm which was attributed to higher carbon and sulphur contents.
The performance of the materials under simulated environmental conditions was investigated by slow strain rate tests. Experiments were conducted on round bar tensile specimens taken from both weld and base material under simulated service conditions in 80 bar hydrogen and 80 bar nitrogen as reference. The materials were tested under continuous rising load until fracture with strain rates of $2.0 \cdot 10^{-5}$ s^{-1} and $2.0 \cdot 10^{-6}$ s^{-1}.
No significant impact of hydrogen on the maximum load measured for both base material and weld specimens was observed. With values above 80% the ductility ratios reveal good resistance of the materials to hydrogen assisted cracking.
Fractographic analysis of the specimens tested in hydrogen atmosphere shows a ductile failure mode for all specimens with no indication for brittle fracture. Small secondary cracks were detected on specimens of the base material of one of the materials. However, no significant impact of hydrogen on the performance of the material in hydrogen atmosphere was observed.
All investigated linepipe materials presented a good resistance to hydrogen embrittlement and hydrogen assisted cracking in the tested environment and are thus considered suitable for hydrogen transmission lines.

REFERENCES

[1] Gräfen, H.; Pöpperling, R.; Schlecker, H.; Schlerkmann, H.; Schwenk, W.: Zur Frage der Schädigung von Hochdruckleitungen durch Wasserstoff und wasserstoffhaltige Gasgemische. Gas Erdgas gwf, 130, Nr. 1, (1989), 16-21

[2] Savakis, S.: Dissertation RWTH Aachen, (1985)

[3] Gräfen, H.; Pöpperling, R.; Schlecker, H.; Schlerkmann, H.; Schwenk, W.: CERT-Untersuchungen an Leitungsrohrstählen über eine Korrosionsgefährdung durch wasserstoffhaltige Gase bei hohen Drücken. Werkstoffe und Korrosion, 39, (1988), 517

[4] Kußmaul, K; Deimel, P.; Sattler, E.; Fischer, H.: Einfluss von Wasserstoff auf ausgewählte Werkstoffe für den Einsatz bei Transport und Speicherung von Wasserstoff. In: Wasserstoff als Energieträger: SFB 270 Universität Stuttgart, Abschlussbericht 1998

[5] Schmitt, G.; Savakis, S.: Untersuchungen zur Schädigung höherfester niedriglegierter Stähle durch Druckwasserstoff bei statischer und dynamischer Beanspruchung. Werkstoffe und Korrosion, 42, (1991), 605-619

[6] Cialone, H.J.; Holbrook, J. H.: Sensitivity of Steels to Degradation in Gaseous Hydrogen. In: Hydrogen Embrittlement: Prevention and Control, ASTM STP962, L. Raymond (Ed.), Philadelphia, (1982), 134-152

[7] Xu, K.; Rana, M.: Tensile and Fracture Properties of Carbon and Low Alloy Steels in High Pressure Hydrogen. In: Effects of Hydrogen on Materials. Proceedings of the 2008 International Hydrogen Conference, B. Somerday, P. Sofronis, R. Jones (Ed.), (2009), 349-356

[8] API SPEC 5L (2012.12): Specification for Line Pipe, 45th Edition

[9] NACE TM0177-2005: Laboratory Testing of Metals for Resistance to Sulfide Stress Cracking and Stress Corrosion Cracking in H_2S Environments. NACE International, Houston, TX, USA (2005)

[10] NACE Standard TM0198-2011: Slow Strain Rate Test Method for Screening Corrosion-Resistant Alloys (CRAs) for Stress Corrosion Cracking in Sour Oilfield Service. NACE International, Houston, TX, USA, (2011)